Υ decay to two charm-quark jets as a probe of the color-octet mechanism

Yu-Jie Zhang[1] and Kuang-Ta Chao[1,2]

[1]*Department of Physics and State Key Laboratory of Nuclear Physics and Technology, Peking University, Beijing 100871, China*

[2]*Center for High Energy Physics, Peking University, Beijing 100871, China*

(Received 21 August 2008; published 20 November 2008)

We calculate the decay rate of bottomonium to two charm-quark jets $\Upsilon \to c\bar{c}$ at the tree level and one-loop level including color-singlet and color-octet $b\bar{b}$ annihilations. We find that the short-distance coefficient of the color-octet piece is much larger than the color-singlet piece, and that the QCD correction will change the end point behavior of the charm quark jet. The color-singlet piece is strongly affected by the one-loop QCD correction. In contrast, the QCD correction to the color-octet piece is weak. Once the experiment can measure the branching ratio and energy distribution of the two charm-quark jets in the Υ decay, the result can be used to test the color-octet mechanism or give a strong constraint on the color-octet matrix elements.

DOI: 10.1103/PhysRevD.78.094017 PACS numbers: 12.38.−t, 12.39.St, 13.20.Gd, 14.40.Gx

I. INTRODUCTION

It is commonly believed that the heavy quark pair production and annihilation decay can be described by perturbative quantum chromodynamics (pQCD) since the heavy quarkonium mass provides a scale that is much larger than $\Lambda_{\rm QCD}$. Because of its nonrelativistic nature, the heavy quarkonium annihilation decay is expected to be described in an effective theory, nonrelativistic quantum chromodynamics (NRQCD) [1]. In the NRQCD factorization formalism, the decay of heavy quarkonium is described by a series of annihilations of the heavy quark pair states and corresponding long-distance matrix elements, which are scaled by the relative velocity v of quark and antiquark in the quarkonium rest frame. The heavy quark pair states can have not only the same quantum numbers as those of the quarkonium, but also other different quantum numbers in color and angular momentum. In particular, the heavy quark pair can be in a color-octet state.

The color-octet scenario seems to acquire some significant successes in describing heavy quarkonium decay and production. But recently, several next-to-leading order (NLO) QCD corrections for the inclusive and exclusive heavy quarkonium production in the color-singlet piece are found to be large and significantly relieve the conflicts between the color-singlet model predictions and experiments. It may imply, though inconclusively, that the color-octet contributions in the production processes are not as big as previously expected, and the color-octet mechanism should be studied more carefully.

The current experimental results on inelastic J/ψ photoproduction at HERA are adequately described by the NLO color-singlet piece [2]. The DELPHI data favor the NRQCD formalism for J/ψ production in $\gamma\gamma \to J/\psi X$, rather than the color-singlet model [3,4]. The large discrepancies in J/ψ production via double $c\bar{c}$ in e^+e^- annihilation at B factories between LO theoretical predictions [5–10] and experimental results [11,12] are probably resolved by including the higher order corrections: NLO QCD corrections and relativistic corrections [13–19]. The NLO QCD corrections in J/ψ and Υ production at the Tevatron and LHC are calculated including the color-singlet piece [20,21] and the color-octet piece [22]. The QCD corrections to polarizations of J/ψ and Υ at the Tevatron and LHC are also calculated [22–24]. The experimental data of polarizations at the Tevatron seem to favor the NLO QCD corrections of the color-singlet piece rather than the color-octet piece. Recent developments and related topics in quarkonium physics can be found in Refs. [25–27].

In order to further test the color-octet mechanism, in this paper we calculate the rate of bottomonium decay into a charm quark pair $\Upsilon \to c\bar{c}$. There have been some works on bottomonium decays and the color-octet mechanism. Fritzsch and Streng calculated the decay rate of Υ into charm at leading order in α_s, $\Upsilon \to ggg^* \to ggc\bar{c}$ [28]. Bigi and Nussinov have taken into account the contribution of $\Upsilon \to gg^*g^* \to gc\bar{c}$ [29]. Barbieri, Caffo, and Remiddi have calculated the decay rates of the P-wave bottomonium states into charm at leading order in α_s [30]. Maltoni and Petrelli calculated the effects of color-octet contributions on the radiative Υ decay [31]. Recently, Bodwin, Braaten, and Kang calculated the inclusive decay rate of χ_b into charmed hadron in the NRQCD framework [32]. Gao, Zhang, and Chao calculated the bottomonium radiative decays to charmonium and light mesons [33,34], as well as Υ radiative decay to light quark jet to test the color-octet mechanism [35]. The S-wave quarkonium decay to light hadrons was calculated up to order v^4 and α_s^3 [36,37]. The exclusive double charmonium production from Υ decay was calculated by Jia [38]. Kang, Kim, Lee, and Yu have calculated the inclusive charm production in $\Upsilon(nS)$ decay [39]. The invariant-mass distribution of $c\bar{c}$ in $\Upsilon(1S) \to c\bar{c} + X$ was also calculated by Chung, Kim, and Lee [40]. And η_b inclusive charm decay was calculated by Hao, Qiao, and Sun [41]. As to experiment, the ARGUS Collaboration searched for charm production in direct decays of the $\Upsilon(1S)$, and found $B^{\rm dir}[\Upsilon(1S) \to D^*(2010)^\pm + X] < 0.019$ [42]. Very recently CLEO has searched for the D^0 production in direct decays of the $\chi_{bJ}(nS)$ ($n = 1, 2$) states [43]. The present investigation for the Υ decay to $c\bar{c}$ pair will hopefully add a new contribution to the test of color-octet mechanism in heavy quarkonium decays.

This paper is organized as follows. In Sec. II, we present the theoretical framework for the decay of $\Upsilon \to c\bar{c}$. In Sec. III, we estimate the color-singlet contributions. In Sec. IV, we include the color-octet contributions. In Sec. V, we discuss the NRQCD matrix elements e.g. $\langle \Upsilon | \mathcal{O}(^3S_{1,8}) | \Upsilon \rangle$ and give a numerical estimation of the color-octet contributions. A summary and discussion are presented in Sec. VI. The detailed and lengthy intermediate steps and formulas in the calculation will be given in the Appendices.

II. THEORETICAL FRAMEWORK

In the framework of NRQCD, the width of Υ decay to $c\bar{c}$ can be written as

$$\Gamma[\Upsilon \to c\bar{c}] = \sum_n \hat{\Gamma}[b\bar{b}(n) \to c\bar{c}] \langle \Upsilon | \mathcal{O}(n) | \Upsilon \rangle, \qquad (1)$$

where n denote quantum numbers including the spin angular momentum S, orbit angular momentum L, total angular momentum J, and the color index 1 or 8. The short-distance coefficients $\hat{\Gamma}[b\bar{b}(n) \to c\bar{c}]$ can be calculated in pQCD, and the long-distance factors $\langle \Upsilon | \mathcal{O}(n) | \Upsilon \rangle$ scale as definite powers of the relative velocity v of quark and antiquark in the quarkonium rest frame [1]. For Υ, the leading order matrix element is $\langle \Upsilon | \mathcal{O}(^3S_{1,1}) | \Upsilon \rangle$, and there are three matrix elements that contribute up to corrections of relative order v^4: $\langle \Upsilon | \mathcal{O}(^1S_{0,8}) | \Upsilon \rangle$, $\langle \Upsilon | \mathcal{O}(^3S_{1,8}) | \Upsilon \rangle$, and $\langle \Upsilon | \mathcal{O}(^3P_{J,8}) | \Upsilon \rangle$. The other matrix elements are of higher order in v.

Feynman diagrams for the color-singlet decay $\Upsilon(b\bar{b}(^3S_{1,1})) \to c\bar{c}$ via a virtual photon (left) and three virtual gluons (right) are shown in Fig. 1. At leading order in α_s, the decay of the color-singlet piece $\Upsilon(b\bar{b}(^3S_{1,1}))$ can proceed through a virtual photon or three virtual gluons. The decay width is of order $\mathcal{O}((\alpha/\pi)^2)$ for the virtual photon, and $\mathcal{O}((\alpha_s/\pi)^6)$ for the three-gluons. So the single photon process is expected to be dominant, and the contribution of the three-gluon process will be roughly estimated in Sec. III. If a soft gluon is allowed to appear in the final state, the order of α_s in the process can be decreased. But the processes of $b\bar{b}(^3S_{1,1}) \to 2g^* + g \to c\bar{c} + g$ and $b\bar{b}(^3S_{1,1}) \to g^* + 2g \to c\bar{c} + 2g$ are infrared (IR) finite [28,29], so the phase space of the soft gluon will bring a suppression factor:

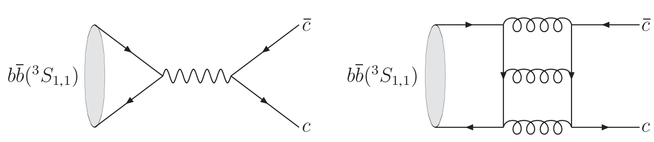

FIG. 1. Feynman diagrams for the color-singlet decay $\Upsilon(b\bar{b}(^3S_{1,1})) \to c\bar{c}$ via a virtual photon (left) and three virtual gluons (right).

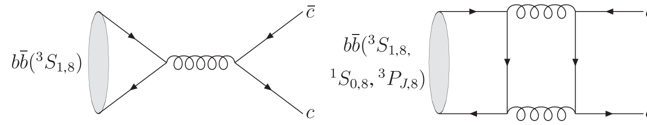

FIG. 2. Feynman diagrams for the color-octet $b\bar{b} \to c\bar{c}$.

$$\frac{d^3k_g}{m_b^2 k_g^0}\bigg|_{k_g^0 < m_b\delta_s} \sim \delta_s^2, \qquad (2)$$

where the factor of m_b^2 is used to balance the dimension, and δ_s is the soft cut. The gluon is regarded as a soft gluon when the energy of the gluon is lower than $m_b\delta_s$. When δ_s is set to, say, 0.2, the corresponding energy cut is about 1 GeV, δ_s^2 is numerically close to α_s/π, so these soft gluon processes are relatively suppressed and should be ignored here.

The decay of the color-octet piece $b\bar{b} \to c\bar{c}$ includes contributions from color-octet $b\bar{b}$ components $^3S_{1,8}$, as well as $^1S_{0,8}$ and $^3P_{J,8}$ in the Υ Fock state expansion. Feynman diagrams for the color-octet $b\bar{b} \to c\bar{c}$ are shown in Fig. 2. The leading order decay width of $b\bar{b}(^3S_{1,8}) \to c\bar{c}$ is of order $\mathcal{O}(\alpha_s^2/\pi^2)$, while processes $b\bar{b}(^1S_{0,8}, {}^3P_{J,8}) \to c\bar{c}$ can only proceed via a loop, and the corresponding decay widths are of order $\mathcal{O}(\alpha_s^4/\pi^4)$. Moreover, since $\langle \Upsilon | \mathcal{O}(^3S_{1,8}) | \Upsilon \rangle \sim \langle \Upsilon | \mathcal{O}(^1S_{0,8}) | \Upsilon \rangle \sim \frac{\langle \Upsilon | \mathcal{O}(^3P_{J,8}) | \Upsilon \rangle}{m_b^2} \sim v^4 \langle \Upsilon | \mathcal{O}(^3S_{1,1}) | \Upsilon \rangle$ according to the velocity scaling rule, the contributions of $\Upsilon(b\bar{b}(^1S_{0,8}, {}^3P_{J,8})) \to c\bar{c}$ can be neglected.

The color-singlet and color-octet contributions will be discussed, respectively, in the next two sections.

III. COLOR-SINGLET PIECE $b\bar{b}(^3S_{1,1}) \to c\bar{c}$

The amplitude of color-singlet piece $b\bar{b}(^3S_{1,1}) \to c\bar{c}$ can be written as [33,35]

$$\begin{aligned}
&\mathcal{A}(b\bar{b}(^3S_{1,1}(2p_b)) \to c(p_c) + \bar{c}(p_{\bar{c}})) \\
&\quad = \sqrt{\frac{\langle \Upsilon | \mathcal{O}(^3S_{1,1}) | \Upsilon \rangle}{2N_c}} \sum_{L_\Upsilon S_{\Upsilon z}} \sum_{s_1 s_2} \sum_{jk} \\
&\qquad \times \langle 1 \mid \bar{3}k; 3j \rangle \langle J_\Upsilon J_{\Upsilon z} \mid L_\Upsilon L_{\Upsilon z}; S_\Upsilon S_{\Upsilon z} \rangle \\
&\qquad \times \langle S_\Upsilon S_{\Upsilon z} \mid s_1; s_2 \rangle \mathcal{A}(b_j(p_b) + \bar{b}_k(p_b) \\
&\quad \to c_l(p_c) + \bar{c}_i(p_{\bar{c}})),
\end{aligned} \qquad (3)$$

where $\langle 1 \mid \bar{3}k; 3j \rangle = \delta_{jk}/\sqrt{N_c}$, $\langle S_\Upsilon S_{\Upsilon z} \mid s_1; s_2 \rangle$, and

$\langle J_\Upsilon J_{\Upsilon z} | L_\Upsilon L_{\Upsilon z}; S_\Upsilon S_{\Upsilon z}\rangle$ are, respectively, the color-SU(3), spin-SU(2), and angular momentum Clebsch-Gordan coefficients for $b\bar{b}$ pairs projecting on appropriate bound states Υ. $\mathcal{A}(b_j(p_b) + \bar{b}_k(p_b) \to c_l(p_c) + \bar{c}_i(p_{\bar{c}}))$ is the amplitude of the process $b_j(p_b) + \bar{b}_k(p_b) \to c_l(p_c) + \bar{c}_i(p_{\bar{c}})$. In the calculation, we use FEYNARTS [44,45] to generate Feynman diagrams and amplitudes, FEYNCALC [46] for the tensor reduction, and LOOPTOOLS [47] for the numerical evaluation of the IR-safe integrals.

The spin projection operators $P_{SS_z}(p, q)$ which describe quarkonium production are expressed in terms of quark and antiquark spinors as [48,49]

$$P_{SS_z}(p, q) = \sum_{s_1,s_2} u\left(\frac{p}{2} + q, s_2\right)\bar{v}\left(\frac{p}{2} - q, s_1\right)\langle s_1; s_2|SS_z\rangle. \tag{4}$$

For the $^3S_1$ state, it is

$$P_{1S_Z}(2p_b, 0) = \frac{1}{2\sqrt{2m_b}}(2\not{p}_b + 2m)\not{\epsilon}(S_z). \tag{5}$$

The spin projection operators which describe the annihilation of quarkonium are the complex conjugate of the corresponding operators for production.

The leading order (LO) color-singlet decay $b\bar{b}(^3S_{1,1}) \to \gamma^* \to c\bar{c}$ is shown in Fig. 1, and the corresponding LO decay width is

$$\Gamma_{\rm LO}[\Upsilon(^3S_{1,1}) \to c\bar{c}] = \frac{4\pi\alpha^2\sqrt{1-r^2}(2+r^2)}{81m_b^2} \times \langle\Upsilon|\mathcal{O}(^3S_{1,1})|\Upsilon\rangle, \tag{6}$$

where $r^2 = m_c^2/m_b^2$. This result is consistent with Refs. [39,40]. Comparing it with the leptonic width

$$\Gamma_{\rm LO}[\Upsilon \to e^+e^-] = \frac{2\pi\alpha^2}{27m_b^2}\langle\Upsilon|\mathcal{O}(^3S_{1,1})|\Upsilon\rangle, \tag{7}$$

we can get

$$\Gamma_{\rm LO}[\Upsilon(^3S_{1,1}) \to c\bar{c}] = \tfrac{4}{3}\Gamma_{\rm LO}[\Upsilon \to e^+e^-] \times (1 + \mathcal{O}(r^2)), \tag{8}$$

where the factor 4/3 comes from the charm quark charge and color factor, and $r^2 \sim 10^{-2}$. If we set $m_b = 4.7$ GeV and $m_c = 1.5$ GeV, the LO decay branching ratio is

$$B_{\rm LO}[\Upsilon(^3S_{1,1}) \to c\bar{c}] = 1.33B_{\rm LO}[\Upsilon \to e^+e^-] = 3.2\%, \tag{9}$$

where $B[\Upsilon \to e^+e^-] = (2.38 \pm 0.11)\%$ is used according to the PDG 2006 version [50].

We next consider the QCD radiative corrections. The Feynman diagrams of one-loop virtual corrections and counterterms are shown in Fig. 3. The renormalization of heavy quark wave function should appear. The on-mass-shell (OS) scheme is chosen for Z_{2b} and Z_{2c} [17]:

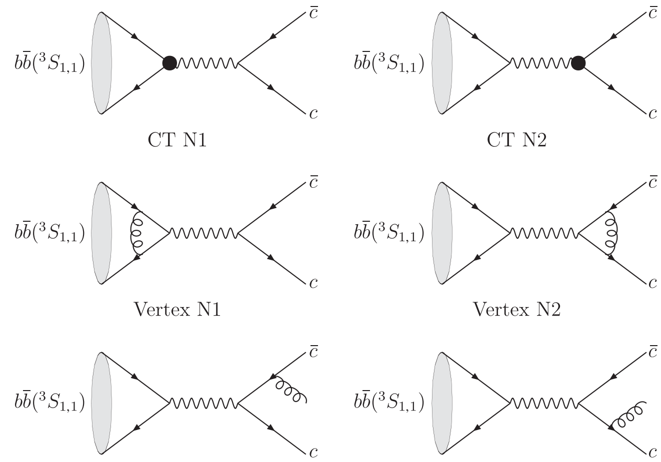

FIG. 3. Feynman diagrams for one-loop QCD corrections with counter terms for $b\bar{b}(^3S_{1,1}) \to \gamma^* \to c\bar{c}$.

$$\delta Z_{2b}^{\rm OS} = -C_F\frac{\alpha_s}{4\pi}\left[\frac{1}{\epsilon_{\rm UV}} + \frac{2}{\epsilon_{\rm IR}} - 3\gamma_E + 3\ln\frac{4\pi\mu^2}{m_b^2} + 4\right] + \mathcal{O}(\alpha_s^2),$$
$$\delta Z_{2c}^{\rm OS} = -C_F\frac{\alpha_s}{4\pi}\left[\frac{1}{\epsilon_{\rm UV}} + \frac{2}{\epsilon_{\rm IR}} - 3\gamma_E + 3\ln\frac{4\pi\mu^2}{m_c^2} + 4\right] + \mathcal{O}(\alpha_s^2), \tag{10}$$

where μ is the renormalization scale, γ_E is the Euler's constant. In this scheme, we need not calculate the correction of external quark legs. We employ the two-loop formula for $\alpha_s(\mu)$,

$$\frac{\alpha_s(\mu)}{4\pi} = \frac{1}{\beta_0 L} - \frac{\beta_1 \ln L}{\beta_0^3 L^2}, \tag{11}$$

where $L = \ln(\mu^2/\Lambda_{\rm QCD}^2)$, and $\beta_1 = (34/3){C_A}^2 - 4C_FT_Fn_f - (20/3)C_AT_Fn_f$ is the two-loop coefficient of the QCD beta function.

The correction to $\Upsilon(b\bar{b}(^3S_{1,1})) \to \gamma^*$ gives a factor of $-\frac{16\alpha_s}{3\pi}$ at $\mathcal{O}(\alpha_s)$. The other part is the correction to $\gamma^* \to c\bar{c}$. If we set $m_c = 0$, then the combined total correction becomes the correction to R, the ratio of cross section of $e^+e^- \to$ light hadrons to that of $e^+e^- \to \mu^+\mu^-$. It give a factor of $\frac{\alpha_s}{\pi}$ at $\mathcal{O}(\alpha_s)$.

Compared with it, the leptonic width of Υ at $\mathcal{O}(\alpha_s)$ becomes the known result:

$$\Gamma_{\rm NLO}[\Upsilon \to e^+e^-] = \frac{2\pi\alpha^2}{27m_b^2}\left(1 - \frac{16\alpha_s}{3\pi}\right)\langle\Upsilon|\mathcal{O}(^3S_{1,1})|\Upsilon\rangle. \tag{12}$$

If the parameters are chosen as $m_b = 4.7$ GeV, $m_c = 1.5$ GeV, and $\alpha_s = 0.220$, then the branching ratio is

$$B_{\rm NLO}[\Upsilon(^3S_{1,1}) \to c\bar{c} + X] = 1.6 B_{\rm NLO}[\Upsilon \to e^+e^-] \approx 3.8\%. \tag{13}$$

When the emitted gluon energy is large, it would form a jet. So a cut to the gluon energy should be introduced to distinguish between $c\bar{c}$ and $c\bar{c}g$ final states. If $E_g < m_b \times \delta_s$, the gluon is considered as soft and the final state is $c\bar{c}$. Otherwise, when $E_g > m_b \times \delta_s$, the final state is $c\bar{c}g$. If we set $\delta_s = 0.15$, then the branching ratio is

$$B_{\rm NLO}[\Upsilon(^3S_{1,1}) \to c\bar{c}] \approx 1.4\%. \tag{14}$$

If we set $\delta_s = 0.10$ and 0.20, then the branching ratio is about 5.4×10^{-3} and 2.0%, respectively.

For the color-singlet piece, the contribution of $\Upsilon(^3S_{1,1}) \to 3g^* \to c\bar{c}$, which is shown on the right-hand side in Fig. 1, has not been calculated so far, and we may have a rough estimate for it. We can use $\Upsilon(^3S_{1,1}) \to 3g$ to give an order of magnitude estimate for the contribution of $\Upsilon(^3S_{1,1}) \to 3g^* \to c\bar{c}$. We have the following order of magnitude estimates:

$$\begin{aligned} &B[\Upsilon(^3S_{1,1}) \to l^+l^-] \propto \left(\frac{\alpha}{\pi}\right)^2, \\ &B[\Upsilon(^3S_{1,1}) \to 3g] \propto \left(\frac{\alpha_s}{\pi}\right)^3, \\ &B[\Upsilon(^3S_{1,1}) \to ggg^* \to ggc\bar{c}] \propto \left(\frac{\alpha_s}{\pi}\right)^4, \\ &B[\Upsilon(^3S_{1,1}) \to 3g^* \to c\bar{c}] \propto \left(\frac{\alpha_s}{\pi}\right)^6. \end{aligned} \tag{15}$$

Comparing the leptonic width with three-gluon width, we get

$$\frac{\Gamma[\Upsilon(^3S_{1,1}) \to l^+l^-]}{\Gamma[\Upsilon(^3S_{1,1}) \to 3g]} \sim \frac{(\frac{\alpha}{\pi})^2}{(\frac{\alpha_s}{\pi})^3} \sim 0.016, \tag{16}$$

which is about one-half of the experimental value of $\frac{\Gamma[\Upsilon(^3S_{1,1}) \to l^+l^-]}{\Gamma[\Upsilon(^3S_{1,1}) \to 3g]} \approx 0.03$ [50], and the closeness of this estimate to the data may suggest that the naive estimate could make sense. Comparing $\Upsilon(^3S_{1,1}) \to 3g^* \to c\bar{c}$ with $\Upsilon(^3S_{1,1}) \to 3g$ and $\Upsilon(^3S_{1,1}) \to \gamma^* \to c\bar{c}$, we can get

$$\frac{\Gamma[\Upsilon(^3S_{1,1}) \to 3g^* \to c\bar{c}]}{\Gamma[\Upsilon(^3S_{1,1}) \to 3g]} \sim \left(\frac{\alpha_s}{\pi}\right)^3 \approx 3 \times 10^{-4}, \tag{17}$$

$$\frac{\Gamma[\Upsilon(^3S_{1,1}) \to 3g^* \to c\bar{c}]}{\Gamma[\Upsilon(^3S_{1,1}) \to \gamma^* \to c\bar{c}]} \sim \frac{\alpha_s^6}{\alpha^2\pi^4} \approx 0.02. \tag{18}$$

From the estimates given in Eqs. (17) and (18), we see that the contribution of $\Upsilon(^3S_{1,1}) \to 3g^* \to c\bar{c}$ is very small and much smaller than that of $\Upsilon(^3S_{1,1}) \to \gamma^* \to c\bar{c}$. Even if the contribution of $\Upsilon(^3S_{1,1}) \to 3g^* \to c\bar{c}$ is underestimated by an order of magnitude in Eqs. (17) and (18), we could still expect that for the decay $\Upsilon(^3S_{1,1}) \to c\bar{c}$ the QED contribution is dominant. Another useful example is the decay rate $\Gamma[\Upsilon(^3S_{1,1}) \to ggc\bar{c}]$, which is of higher order in α_s than $\Gamma[\Upsilon(^3S_{1,1}) \to ggg]$, and is given in Ref. [39]. From their estimate we can get $\frac{\Gamma[\Upsilon(^3S_{1,1}) \to ggc\bar{c}]}{\Gamma[\Upsilon(^3S_{1,1}) \to ggg]} = 0.029$, which is also of the same order of magnitude as, but even smaller than, our naive estimate:

$$\frac{\Gamma[\Upsilon(^3S_{1,1}) \to ggc\bar{c}]}{\Gamma[\Upsilon(^3S_{1,1}) \to ggg]} \sim \left(\frac{\alpha_s}{\pi}\right) \approx 0.071. \tag{19}$$

This might imply that the naive estimates given in Eq. (15) as well as in Eq. (18) might be tenable in estimating the rates of higher order processes by order of magnitude. So, based on the rough estimate given in Eq. (18) for the contributions of the color-singlet piece to the $\Upsilon(^3S_{1,1}) \to c\bar{c}$ process, we assume that, as an approximation, the contribution of $\Upsilon(^3S_{1,1}) \to 3g^* \to c\bar{c}$ can be neglected, and only $\Upsilon(^3S_{1,1}) \to \gamma^* \to c\bar{c}$ will be taken into consideration.

IV. COLOR-OCTET PIECE $b\bar{b}(^3S_{1,8}) \to c\bar{c}$

The amplitude of color-octet piece $b\bar{b}(^3S_{1,8}) \to c\bar{c}$ can be written as [33,35]

$$\begin{aligned} &\mathcal{A}(b\bar{b}(^3S_{1,8}(2p_b)) \to c(p_c) + \bar{c}(p_{\bar{c}})) \\ &\quad = \sqrt{\langle\Upsilon|\mathcal{O}(^3S_{1,8})|\Upsilon\rangle} \sum_{L_{\Upsilon z} S_{\Upsilon z}} \sum_{s_1 s_2} \sum_{jk} \\ &\qquad \times \langle 8a \mid \bar{3}k; 3j\rangle \langle JJ_z \mid LL_z; SS_z\rangle \\ &\qquad \times \langle SS_z \mid s_1; s_2\rangle \mathcal{A}(b_j(p_b) + \bar{b}_k(p_b) \\ &\quad \to c_l(p_c) + \bar{c}_i(p_{\bar{c}})), \end{aligned} \tag{20}$$

where $\langle 8a \mid \bar{3}k; 3j\rangle = \sqrt{2}T^a_{jk}$, and other expressions are similar to the color-singlet piece.

The Born diagram of $b\bar{b}(^3S_{1,8}) \to c\bar{c}$ is shown in Fig. 2. It is also calculated in Ref. [32]. The leading order width is

$$\Gamma_{\rm LO}[\Upsilon(^3S_{1,8}) \to c\bar{c}] = \frac{\alpha_s^2\sqrt{1-r^2}(2+r^2)\pi}{6m_b^2} \times \langle\Upsilon|\mathcal{O}(^3S_{1,8})|\Upsilon\rangle. \tag{21}$$

We further calculate the next-to-leading order (NLO) corrections. The Feynman diagrams for NLO virtual corrections with counterterms in the color-octet piece $b\bar{b}(^3S_{1,8}) \to c\bar{c}$ are shown in Fig. 4. The Feynman diagrams for NLO real corrections in the color-octet piece $b\bar{b}(^3S_{1,8}) \to c\bar{c}$ are shown in Fig. 5. The renormalization of heavy quark wave function, gluon wave function, and coupling constant should appear here. Z_{2b} and Z_{2c} are given in Eq. (10). For Z_3 and Z_g, we choose the modified minimal-subtraction ($\overline{\rm MS}$) scheme [17]:

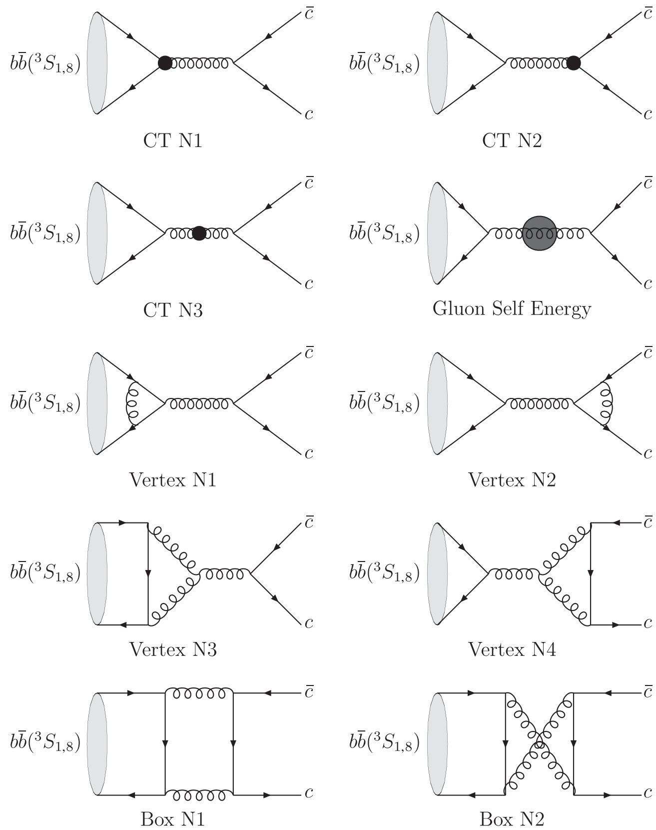

FIG. 4. Feynman diagrams for next-to-leading order virtual corrections with counter terms in the color-octet piece $b\bar{b}(^3S_{1,8}) \to c\bar{c}$.

$$\delta Z_3^{\overline{\rm MS}} = \frac{\alpha_s}{4\pi}(\beta_0 - 2C_A)\left[\frac{1}{\epsilon_{\rm UV}} - \gamma_E + \ln(4\pi)\right] + \mathcal{O}(\alpha_s^2),$$
$$\delta Z_g^{\overline{\rm MS}} = -\frac{\beta_0}{2}\frac{\alpha_s}{4\pi}\left[\frac{1}{\epsilon_{\rm UV}} - \gamma_E + \ln(4\pi)\right] + \mathcal{O}(\alpha_s^2). \quad (22)$$

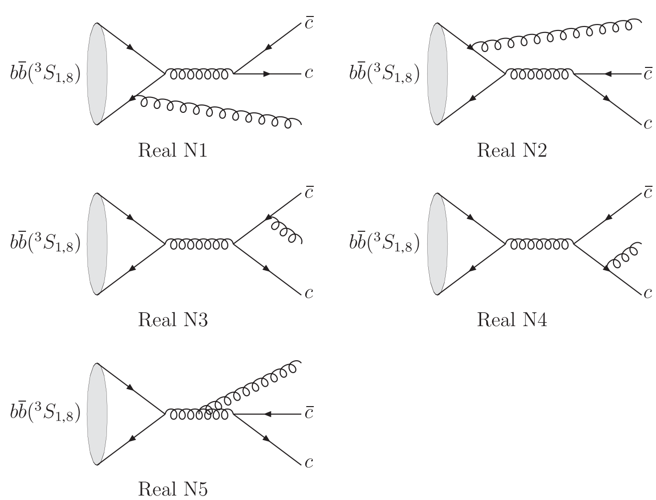

FIG. 5. Feynman diagrams for next-to-leading order real corrections in the color-octet piece $b\bar{b}(^3S_{1,8}) \to c\bar{c}$.

The parameters are chosen as $m_b = 4.7$ GeV, $m_c = 1.5$ GeV, $n_f = 4$, $\Lambda_{\rm QCD}^{(4)} = 338$ MeV, $\mu = m_b$, and then $\alpha_s = 0.220$. So we can get the leading order result:

$$B_{\rm LO}[\Upsilon(^3S_{1,8}) \to c\bar{c}] = 42 \times \frac{\langle\Upsilon|\mathcal{O}(^3S_{1,8})|\Upsilon\rangle}{\rm GeV^3}. \quad (23)$$

The total NLO result is

$$B_{\rm NLO}[\Upsilon(^3S_{1,8}) \to c\bar{c} + X] = 53 \times \frac{\langle\Upsilon|\mathcal{O}(^3S_{1,8})|\Upsilon\rangle}{\rm GeV^3}. \quad (24)$$

If we set the soft cut $\delta_s = 0.15$, then the NLO result is

$$B_{\rm NLO}[\Upsilon(^3S_{1,8}) \to c\bar{c}] = 41 \times \frac{\langle\Upsilon|\mathcal{O}(^3S_{1,8})|\Upsilon\rangle}{\rm GeV^3}. \quad (25)$$

If we set the soft cut $\delta_s = 0.10$ and 0.20, then the branching ratio is $37 \times \frac{\langle\Upsilon|\mathcal{O}(^3S_{1,8})|\Upsilon\rangle}{\rm GeV^3}$ and $44 \times \frac{\langle\Upsilon|\mathcal{O}(^3S_{1,8})|\Upsilon\rangle}{\rm GeV^3}$, respectively.

From the above expressions, we see that the short-distance coefficient for this color-octet process is large, and this color-octet process may make a significant contribution to the Υ decay to two charm-quark jet. The numerical estimate will be given in the next section.

The color-octet pieces $b\bar{b}(^3P_{J,8})$ and $b\bar{b}(^1S_{0,8})$ also contribute to the charm quark jet production through $c\bar{c}g$, where the gluon is soft. The $b\bar{b}(^3P_{J,8}) \to c\bar{c}g$ is IR divergent, and it should be absorbed into the matrix element $\langle\Upsilon|\mathcal{O}(^3S_{1,8})|\Upsilon\rangle$ [1]:

$$\langle\Upsilon|\mathcal{O}(^3S_{1,8})|\Upsilon\rangle_1 = \langle\Upsilon|\mathcal{O}^H(^3S_{1,8})|\Upsilon\rangle_0\left[1 + \left(C_F - \frac{C_A}{2}\right)\frac{\pi\alpha_s}{2v}\right] + \frac{4\alpha_s}{3\pi m_b^2}\left(\frac{4\pi\mu^2}{\lambda^2}\right)^\epsilon \exp(-\epsilon\gamma_E) \times\left(\frac{1}{\epsilon_{\rm UV}} - \frac{1}{\epsilon_{\rm IR}}\right)\sum_{J=0}^{2} B_F\langle\Upsilon|\mathcal{O}(^3P_{J,8})|\Upsilon\rangle, \quad (26)$$

where the Coulomb term of $\langle\Upsilon|\mathcal{O}(^3S_{1,8})|\Upsilon\rangle_1$ is canceled by the virtual correction, the IR divergent terms is canceled by $b\bar{b}(^3P_{J,8}) \to c\bar{c}g$, and the UV divergent term gives the running of matrix element. If we choose the matrix element renormalization scale as m_b, then we find the branching ratio of $b\bar{b}(^3P_{J,8})$ and $b\bar{b}(^1S_{0,8})$ decays into $c\bar{c}g$ at order of α_s^3 to be

$$B[\Upsilon(^1S_{0,8}) \to c\bar{c} + X] = 2.8 \times \frac{\langle\Upsilon|\mathcal{O}(^1S_{0,8})|\Upsilon\rangle}{\rm GeV^3},$$
$$B[\Upsilon(^3P_{J,8}) \to c\bar{c} + X] = 0.61 \times \frac{\langle\Upsilon|\mathcal{O}(^3P_{0,8})|\Upsilon\rangle}{\rm GeV^5}. \quad (27)$$

Since $\langle\Upsilon|\mathcal{O}(^1S_{0,8})|\Upsilon\rangle$, $\langle\Upsilon|\mathcal{O}(^3S_{1,8})|\Upsilon\rangle$, and $\langle\Upsilon|\mathcal{O}(^3P_{J,8})|\Upsilon\rangle/m_b^2$ are of the same order, we can ignore

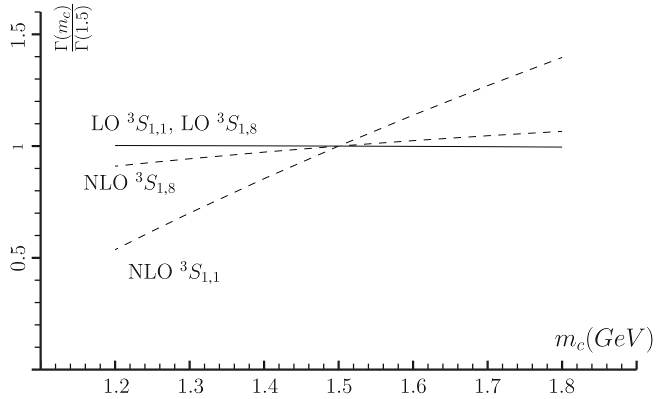

FIG. 6. Decay widths of the color-singlet piece and color-octet piece $b\bar{b}(^3S_1) \to c\bar{c}$ rescaled by the corresponding value at $m_c =$ 1.5 GeV as functions of the charm quark mass m_c. Here $\Lambda =$ 0.338 GeV, $m_b = 4.7$ GeV, $\mu = m_b$, and the soft cut $\delta_s =$ 0.15. LO means leading order, and NLO means next-to-leading order. $^3S_{1,1}$ means the ratio $\Gamma[b\bar{b}(^3S_{1,1} \to c\bar{c}](m_c)/\Gamma[b\bar{b}(^3S_{1,1} \to c\bar{c}](m_c = 1.5\text{ GeV})$ in the color-singlet piece, and $^3S_{1,8}$ means the corresponding ratio in the color-octet piece.

the contribution of $b\bar{b}(^3P_{J,8})$ and $b\bar{b}(^1S_{0,8})$, as compared with the $b\bar{b}(^3S_{1,8})$ contribution given in Eq. (24).

The dependence of the leading order and next-to-leading order decay widths in the color-singlet and color-octet pieces $b\bar{b} \to c\bar{c}$ on the charm quark is shown in Fig. 6. The dependence of the LO result on the charm quark mass is weak and the same for the color-singlet and color-octet pieces. The reason can be found in Eq. (6) and Eq. (21). If we choose $m_c = 1.5 \pm 0.2$ GeV, the ratio is about 1 ± 0.003 at LO in α_s, $1^{+0.27}_{-0.30}$ at NLO for the color-singlet piece, and $1^{+0.046}_{-0.057}$ at NLO for the color-octet piece.

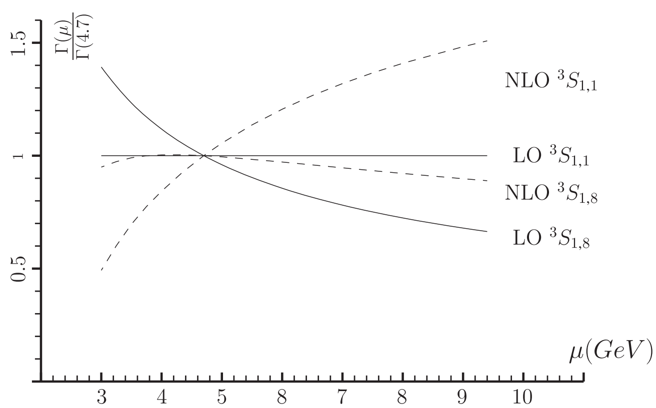

FIG. 7. Decay widths of the color-singlet piece and color-octet piece $b\bar{b}(^3S_1) \to c\bar{c}$ rescaled by the corresponding value at $\mu = m_b$ as functions of the renormalization scale μ. Here $\Lambda =$ 0.338 GeV, $m_b = 4.7$ GeV, $m_c = 1.5$ GeV, and the soft cut $\delta_s = 0.15$. LO means leading order, and NLO means next-to-leading order. $^3S_{1,1}$ means the ratio of $\Gamma[b\bar{b}(^3S_{1,1} \to c\bar{c}] \times (\mu)/\Gamma[b\bar{b}(^3S_{1,1} \to c\bar{c}](\mu = m_b)$ in the color-singlet piece, and $^3S_{1,8}$ means the corresponding ratio in the color-octet piece.

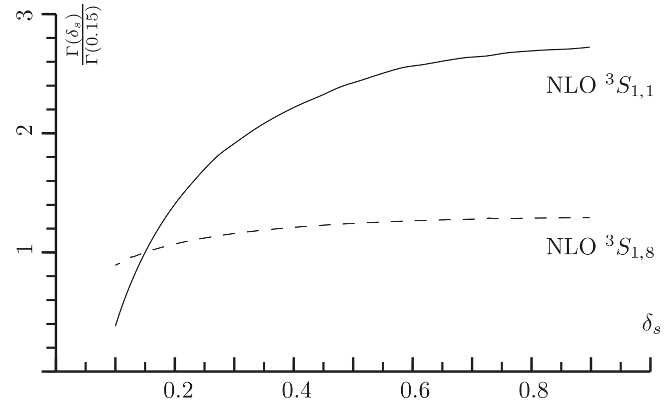

FIG. 8. Decay widths of the color-singlet piece and color-octet piece $b\bar{b}(^3S_1) \to c\bar{c}$ rescaled by the corresponding value at $\delta_s =$ 0.15 as functions of the soft cut δ_s. Here $\Lambda = 0.338$ GeV, $m_b =$ 4.7 GeV, $\mu = m_b$, and $m_c = 1.5$ GeV. NLO means next-to-leading order. $^3S_{1,1}$ means the ratio of $\Gamma[b\bar{b}(^3S_{1,1} \to c\bar{c}] \times (\delta_s)/\Gamma[b\bar{b}(^3S_{1,1} \to c\bar{c}](\delta_s = 0.15)$, and $^3S_{1,8}$ means the corresponding ratio in the color-octet piece.

The dependence of the leading order and next-to-leading order decay widths in the color-singlet and color-octet pieces $b\bar{b} \to c\bar{c}$ on the renormalization scale μ is shown in Fig. 7. The LO color-singlet result is independent of the renormalization scale. As it is shown in the curve of NLO $^3S_{1,8}$, we choose $\mu = m_b$ for the principle of minimum sensitivity (PMS) [51].

The dependence of the next-to-leading order decay widths in the color-singlet and color-octet pieces $b\bar{b} \to c\bar{c}$ on the soft cut δ_s is shown in Fig. 8. The LO result is independent of the soft cut δ_s. The NLO color-singlet result is rather sensitive to δ_s, whereas the NLO color-octet result is insensitive to δ_s.

V. COLOR-OCTET MATRIX ELEMENTS

The color-singlet matrix element $\langle\Upsilon|\mathcal{O}(^3S_{1,1})|\Upsilon\rangle$ can be extracted from the Υ leptonic decay width. Using Eq. (12), we get

$$\langle\Upsilon|\mathcal{O}(^3S_{1,1})|\Upsilon\rangle = 3.8\text{ GeV}^3. \tag{28}$$

On the other hand, large uncertainty is related to the color-octet matrix element $\langle\Upsilon|\mathcal{O}(^3S_{1,8})|\Upsilon\rangle$. According to the velocity scaling rule and taking $v^2 = 0.08$, we might naively have

$$\langle\Upsilon|\mathcal{O}(^3S_{1,8})|\Upsilon\rangle \approx \frac{v^4}{2N_c}\langle\Upsilon|\mathcal{O}(^3S_{1,1})|\Upsilon\rangle = 4.1 \times 10^{-3}\text{ GeV}^3. \tag{29}$$

Using Eq. (24), we would get

$$B_{\rm NLO}[\Upsilon(^3S_{1,8}) \to c\bar{c} + X] = 21\%. \tag{30}$$

For the light quark $q = u, d, s$, we have

$$B_{\rm NLO}[\Upsilon(^3S_{1,8}) \to q\bar{q} + X] = B_{\rm NLO}[\Upsilon(^3S_{1,8}) \to c\bar{c} + X] \times (1 + \mathcal{O}(r^2)). \quad (31)$$

So Υ decay through $b\bar{b}(^3S_{1,8})$ would have a very large branching ratio, say about 80%. Apparently, the color-octet matrix element estimated in this naive way from the velocity scaling rule is greatly overestimated, even by an order of magnitude.

Another approach to determine the matrix element is the lattice QCD calculations. The lattice calculation in Ref. [52] gives

$$\langle\Upsilon|\mathcal{O}(^3S_{1,8})|\Upsilon\rangle \approx 8.1 \times 10^{-5}\langle\Upsilon|\mathcal{O}(^3S_{1,1})|\Upsilon\rangle = 3.1 \times 10^{-4}\ \mathrm{GeV}^3. \quad (32)$$

If we set the soft cut $\delta_s = 0.15$, then the next-to-leading order result is

$$B_{\rm NLO}[\Upsilon(^3S_{1,8}) \to c\bar{c}] = 1.3\%. \quad (33)$$

If we set the soft cut $\delta_s = 0.10$ and $\delta_s = 0.20$, the branching ratio is 1.1% and 1.4%, respectively.

From the above numerical results and Eq. (24), we see that since the short-distance coefficient for the color-octet contribution to the $\Upsilon \to c\bar{c}$ decay is large, this process is sensitive to the value of the color-octet matrix element, and may therefore serve as a useful test ground of the color-octet mechanism.

Moreover, the next-to-leading order QCD correction in the color-singlet piece is much stronger than that in the color-octet piece, and the color-singlet contribution shows a strong sensitivity to the soft cut δ_s, whereas the color-octet result does not. These differences between the color-singlet and color-octet contributions will also be significant in clarifying the issue about the color-octet mechanism. Once the experiment can measure the branching ratio and energy distribution of the charm quark jet in the Υ decay, the result can be used to test the color-octet mechanism or give a strong constraint on the color-octet matrix elements.

VI. SUMMARY AND DISCUSSION

We calculate the decay rate of bottomonium to two charm-quark jets $\Upsilon \to c\bar{c}$ at the tree level and one-loop level including color-singlet and color-octet $b\bar{b}$ annihilations. We find that the short-distance coefficient of the color-octet piece is much larger than the color-singlet piece, and that the QCD correction will change the end point behavior of the charm quark jet. The color-singlet piece is strongly affected by the one-loop QCD correction. In contrast, the QCD correction to the color-octet piece is weak. Once the experiment can measure the branching ratio and energy distribution of the two charm-quark jets in the Υ decay, the result can be used to test the color-octet mechanism or give a strong constraint on the color-octet matrix elements.

After our work was completed [53], a paper appeared [39] in which Kang, Kim, Lee, and Yu calculated the inclusive charm production in $\Upsilon(nS)$ decay. They focused on the inclusive charm production of the color-singlet piece at leading order in the strong coupling constant α_s. We focused on the $c\bar{c}$ final state and the color-octet mechanism. The $c\bar{c}$ final state is essentially the two-charm-jet process. And we have calculated the next-to-leading order QCD corrections in both color-singlet and color-octet pieces. Our leading order result of $\Upsilon \to \gamma^* \to c\bar{c}$ is consistent with their result [39].

ACKNOWLEDGMENTS

We thank C. Meng for useful discussions. This work was supported in part by the National Natural Science Foundation of China (No. 10421503, No. 10675003), and also by China Postdoctoral Science Foundation (No. 20070420011).

APPENDIX A: THE SCALAR FUNCTIONS

The scalar functions that appear in the virtual corrections are listed in this Appendix. There are UV, IR, and Coulomb singularities in the scalar functions. The UV and IR singularities are regularized with $D = 4 - 2\epsilon$ space-time dimension. The exchange of longitudinal gluon between massive quarks in vertex N1 in Figs. 3 and 4 leads to a Coulomb singularity $\sim\pi^2/v$, where $v = \sqrt{-(p_b - p_{\bar{b}})^2}/m_b$ is the relative velocity between b and $\bar{b}$ in the meson rest frame ($v = |\vec{p}_b - \vec{p}_{\bar{b}}|/m_b$). The Coulomb singularities should be canceled by that in the matrix elements (see, e.g., [16,17]).

Since the imaginary part of the integrals will disappear in the final result, only the real parts are given. The external particles are taken to be on-mass-shell, $p_b^2 = p_{\bar{b}}^2 = m_b^2$, $p_c^2 = p_{\bar{c}}^2 = m_c^2$, $p_b \cdot p_c = p_b \cdot p_{\bar{c}} = m_b^2$, and $p_c \cdot p_{\bar{c}} = 2m_b^2 - m_c^2$.

The scalar one-point function is defined as

$$A_0(m^2) = \mu^{4-D}\int \frac{d^Dq}{(2\pi)^D}\frac{1}{q^2 - m^2} = iC_\epsilon(m)m^2\left[\frac{1}{\epsilon} + 1\right], \quad (A1)$$

where

$$C_\epsilon(m) = \frac{1}{16\pi^2}e^{-\epsilon(\gamma_E - \ln 4\pi)}\left(\frac{\mu^2}{m^2}\right)^\epsilon \quad (A2)$$

and $D = 4 - 2\epsilon$.

The scalar two-point function is defined as

$$B_0(p, m_0, m_1) = \mu^{4-D}\int \frac{d^Dq}{(2\pi)^D} \times \frac{1}{[q^2 - m_0^2][(q + p)^2 - m_1^2]}. \quad (A3)$$

Four different types of two-point functions appear in the calculation of the virtual corrections:

$$B_0(p_b, 0, m_b) = B_0(2p_b, m_b, m_b) = iC_\epsilon(m_b)\left[\frac{1}{\epsilon} + 2\right] \tag{A4}$$

$$B_0(p_c, 0, m_c) = B_0(p_{\bar{c}}, 0, m_c) = iC_\epsilon(m_c)\left[\frac{1}{\epsilon} + 2\right] \tag{A5}$$

$$B_0(2p_b, m_c, m_c) = iC_\epsilon(m_c)\left[\frac{1}{\epsilon} + 2 + \beta \ln\left(\frac{1-\beta}{1+\beta}\right)\right] \tag{A6}$$

$$B_0(p_c - p_b, m_c, m_b) = iC_\epsilon(m_c)\left[\frac{1}{\epsilon} + 2 + \frac{1}{\beta} \ln\left(\frac{1-\beta}{1+\beta}\right)\right] \tag{A7}$$

$$B_0(2p_b, 0, 0) = iC_\epsilon(m_c)\left[\frac{1}{\epsilon} - \ln\left(\frac{4m_b^2}{m_c^2}\right) + 2\right]. \tag{A8}$$

Here and below we will use the shorthand notation $\beta = \sqrt{1-r^2} = \sqrt{1 - m_c^2/m_b^2}$.

The scalar three-point function is defined as

$$C_0(p_1, p_2, m_0, m_1, m_2) = \mu^{4-D}\int \frac{d^D q}{(2\pi)^D} \frac{1}{[q^2 - m_0^2][(q+p_1)^2 - m_1^2][(q+p_2)^2 - m_2^2]}. \tag{A9}$$

The following types of three-point functions appear in the virtual corrections:

$$C_0(p_c, -p_{\bar{c}}, 0, m_c, m_c) = \frac{iC_\epsilon(m_c)}{4m_b^2\beta}\left[\frac{1}{\epsilon}\ln x_\beta - 2\ln x_\beta \ln(1-x_\beta) - 2\mathrm{Li}_2(x_\beta) + \frac{1}{2}\ln^2 x_\beta - 4\zeta(2)\right] \tag{A10}$$

$$C_0(p_c, p_b, 0, m_c, m_b) = \frac{iC_\epsilon(\sqrt{m_c m_b})}{4m_c m_b \chi/(\chi^2-1)}\left[\frac{1}{\epsilon}\ln\left(\frac{1-\chi}{\chi+1}\right) + \frac{1}{2}\ln^2\left(\frac{1-\chi}{\chi+1}\right) - \frac{\ln^2 r}{2} - 2\ln\left(\frac{4\chi}{(\chi+1)^2}\right)\ln\left(\frac{1-\chi}{\chi+1}\right)\right.$$
$$\left. - \mathrm{Li}_2\left(\frac{(\chi-1)^2}{(\chi+1)^2}\right) - \mathrm{Li}_2\left(1 + \frac{r(\chi-1)}{\chi+1}\right) - \mathrm{Li}_2\left(1 + \frac{\chi-1}{r(\chi+1)}\right) + \frac{\pi^2}{6}\right] \tag{A11}$$

$$C_0(p_c, -p_{\bar{c}}, m_c, 0, 0) = i\frac{1}{4(4\pi)^2 m_b^2 \beta}\left[2\mathrm{Li}_2(-x_\beta) + \frac{1}{2}\ln^2 x_\beta + \zeta(2)\right] \tag{A12}$$

$$C_0(p_b, -p_b, m_b, 0, 0) = i\frac{\ln 2}{(4\pi)^2 m_b^2}, \tag{A13}$$

where $x_\beta = (1-\beta)/(1+\beta)$, $\zeta(2) = \pi^2/6$, $r = m_c/m_b$, and $\chi = \sqrt{(1-r)/(1+r)}$. There is another scalar three-point function that is IR and Coulomb divergent,

$$C_0(p_b, -p_{\bar{b}}, 0, m_b, m_b) = -i\frac{C_\epsilon(m_b)}{2m_b^2}\left[\frac{1}{\epsilon} + \frac{\pi^2}{v} - 2 + \mathcal{O}(\epsilon)\right], \tag{A14}$$

where $v = \sqrt{-(p_b - p_{\bar{b}})^2}/m_b$. In the meson rest frame, we have $v = |\vec{p}_b - \vec{p}_{\bar{b}}|/m_b$.

The scalar four-point function is defined by

$$D_0(p_1, p_2, p_3, m_0, m_1, m_2, m_3) = \mu^{4-D}\int \frac{d^D q}{(2\pi)^D} \frac{1}{[q^2 - m_0^2][(q+p_1)^2 - m_1^2][(q+p_2)^2 - m_2^2][(q+p_3)^2 - m_3^2]}. \tag{A15}$$

There are three different types of four-point functions:

$$D_0(p_b, p_b - p_c, -p_b, m_b, 0, m_c, 0) = \frac{iC_\epsilon(\sqrt{m_c m_b})}{8m_b^4}\left\{\frac{(\chi^2-1)}{r\chi}\left[\frac{1}{\epsilon}\ln\left(\frac{1-\chi}{\chi+1}\right) + \frac{1}{2}\ln^2\left(\frac{1-\chi}{\chi+1}\right) - \frac{\ln^2 r}{2} - 2\ln\left(\frac{4\chi}{(\chi+1)^2}\right)\right.\right.$$
$$\left. \times \ln\left(\frac{1-\chi}{\chi+1}\right) - \mathrm{Li}_2\left(\frac{(\chi-1)^2}{(\chi+1)^2}\right) - \mathrm{Li}_2\left(1 + \frac{r(\chi-1)}{\chi+1}\right) - \mathrm{Li}_2\left(1 + \frac{\chi-1}{r(\chi+1)}\right) + \frac{\pi^2}{6}\right]$$
$$\left. - \frac{1}{\beta}\left[2\mathrm{Li}_2(-x_\beta) + \frac{1}{2}\ln^2 x_\beta + \zeta(2)\right]\right\}, \tag{A16}$$

The IR and Coulomb singularities can be regularized by the gluon mass m_g. The relation between the gluon mass m_g regularization and the dimensional regularization for IR singularity is

$$\ln\left(\frac{\lambda^2}{m^2}\right) \Leftrightarrow \frac{1}{\epsilon} - \gamma_E + \ln\frac{4\pi\mu^2}{m^2}. \tag{A17}$$

The relation between different regularization schemes for the Coulomb singularity is

$$\frac{2\pi m}{\lambda} \Leftrightarrow \frac{\pi^2}{v}. \tag{A18}$$

Equations (A17) and (A18) are consistent with Ref. [2].

APPENDIX B: REAL CORRECTIONS AND THE THREE-BODY PHASE SPACE

For the real corrections, the process $\Upsilon(2p_b) \to c(p_c) + \bar{c}(p_{\bar{c}}) + g(k)$ is a three-body decay process. Similar to the method in Ref. [47], we can write down the Lorentz-invariant phase space

$$dPS_3(2p_b; k, p_c, p_{\bar{c}}) = \frac{d^3k}{(2\pi)^3 2k^0}\frac{d^3p_c}{(2\pi)^3 2p_c^0}\frac{d^3p_{\bar{c}}}{(2\pi)^3 2p_{\bar{c}}^0} \times (2\pi)^4\delta^4(2p_b - k - p_c - p_{\bar{c}}). \tag{B1}$$

Introduce the identities

$$\frac{d^3p_i}{2p_i^0} = d^4p_i\delta(p_i^2 - m_i^2) = \frac{|\vec{p}_i|^2 d|\vec{p}_i| d\Omega_i}{2p_i^0} = \frac{|\vec{p}_i| dp_i^0 d\Omega_i}{2}, \tag{B2}$$

where m_i is the mass of particle i, and $d\Omega_i$ is the direction of particle i in the three dimension space. Then we can rewrite $dPS_3(2p_b; k, p_c, p_{\bar{c}})$:

$$\begin{aligned} dPS_3 &= \frac{|\vec{k}||\vec{p}_c|}{4(2\pi)^5} dk^0 d\Omega_g dp_c^0 d\Omega_c d^4p_{\bar{c}}\delta(p_{\bar{c}}^2 - m_{\bar{c}}^2) \\ &\quad \times \delta^4(2p_b - k - p_c - p_{\bar{c}}) \\ &= \frac{|\vec{k}||\vec{p}_c|}{4(2\pi)^5} dk^0 d\Omega_g dp_c^0 d\Omega_c \delta[(2p_b - k - p_c)^2 - m_{\bar{c}}^2]. \end{aligned} \tag{B3}$$

We define the momenta in the rest frame of the Υ,

$$\begin{aligned} 2p_b &= (2m_b, 0, 0, 0) \\ p_c &= (p_c^0, |\vec{p}_c|\sin\theta, 0, |\vec{p}_c|\cos\theta) \\ k &= (k^0, 0, 0, |\vec{k}|) \\ p_{\bar{c}} &= (p_{\bar{c}}^0, -|\vec{p}_c|\sin\theta, 0, -|\vec{k}| - |\vec{p}_c|\cos\theta), \end{aligned} \tag{B4}$$

where θ is the angular between g and c, and $|\vec{p}_i| = \sqrt{(p_i^0)^2 - m_i^2}$. Then $d\Omega_g$ gives a factor 4π, and $d\Omega_c = d\cos\theta d\phi$ and $d\phi$ gives a factor 2π. So we have

$$dPS_3 = \frac{|\vec{k}||\vec{p}_c|}{2(2\pi)^3} dk^0 dp_c^0 d\cos\theta\delta[(2p_b - k - p_c)^2 - m_{\bar{c}}^2]. \tag{B5}$$

Then we use the δ function to remove θ in the integral with

$$\begin{aligned} (2p_b - k - p_c)^2 - m_{\bar{c}}^2 &= (\sqrt{s} - k^0 - p_c^0)^2 \\ &\quad - (|\vec{k}|^2 + |\vec{p}_c|^2 + 2|\vec{k}||\vec{p}_c|\cos\theta) \\ &\quad - m_{\bar{c}}^2 \\ &\equiv f(\cos\theta) \end{aligned} \tag{B6}$$

and

$$\left|\frac{df(\cos\theta)}{d\cos\theta}\right| = 2|\vec{k}||\vec{p}_c|, \tag{B7}$$

and get

$$\cos\theta = \frac{(\sqrt{s} - k^0 - p_c^0)^2 - |\vec{k}|^2 - |\vec{p}_c|^2 - m_{\bar{c}}^2}{2|\vec{k}||\vec{p}_c|}, \tag{B8}$$

and

$$dPS_3 = \frac{1}{4(2\pi)^3} dk^0 dp_c^0. \tag{59}$$

To determine the limits of integration, we employ the restriction of $|\cos\theta| \le 1$ and $p_i^0 \ge m_i^0$, then we get

$$(k^0)^{\min} = m_g, \qquad (k^0)^{\max} = m_b - \frac{(m_c + m_{\bar{c}})^2 - m_g^2}{4m_b}, \tag{B10}$$

and

$$\begin{aligned} (p_c^0)^{\max,\min} &= \frac{1}{2\tau}\left[\sigma(\tau + m_+m_-) \pm |\vec{k}|\sqrt{(\tau - m_+^2)(\tau - m_-^2)}\right] \\ \sigma &= \sqrt{s} - k^0, \quad \tau = \sigma^2 - |\vec{k}|^2, \\ m_\pm &= m_c \pm m_{\bar{c}}. \end{aligned} \tag{B11}$$

Here we keep the gluon mass m_g for massive gluon regularization. There is a soft divergence in the real corrections, so we should introduce a soft cut E_s for the gluon. Then the phase space is divided into two regions:

$$dPS_3 = dPS_3^{\rm soft}|_{k^0<E_s} + dPS_3^{\rm hard}|_{k^0>E_s}. \tag{B12}$$

The hard region can be integrated in four dimensions or with massless gluon. The phase space in the soft region is

$$dPS_3^{\rm soft}|_{k^0<E_s} = dPS_2\int d\Omega_g^{D-1}\int^{E_s}\frac{|\vec{k}|^{D-3}}{2(2\pi)^{D-1}}dk^0. \tag{B13}$$

The decay amplitude of the color-singlet process can be written as

$$\begin{aligned}\mathcal{A}^{\text{real}}(b\bar{b}(^3S_{1,1}(2p_b)) \to c(p_c) + \bar{c}(p_{\bar{c}}) + g(k))|_{k^0<E_s} &= g_s\mu^\epsilon \varepsilon^a_{*\mu}(k)\mathcal{A}^{\text{Born}}(b\bar{b}(^3S_{1,1}(2p_b) \\ &\quad \to c(p_c) + \bar{c}(p_{\bar{c}})) \\ &\quad \otimes T^a\left(\frac{p_c^\mu}{p_c\cdot k} - \frac{p_{\bar{c}}^\mu}{p_{\bar{c}}\cdot k}\right)\end{aligned} \tag{B14}$$

and

$$|\mathcal{A}^{\text{real}}(^3S_{1,1})|_{k^0<E_s}|^2 = |\mathcal{A}^{\text{Born}}(^3S_{1,1})|^2 g_s^2\mu^{2\epsilon}\tfrac{4}{3} \times (\mathcal{I}_{cc} - 2\mathcal{I}_{c\bar{c}} + \mathcal{I}_{\bar{c}\bar{c}}), \tag{B15}$$

where

$$\mathcal{I}_{ij} = -\frac{p_i\cdot p_j}{p_i\cdot k p_j\cdot k}. \tag{B16}$$

The decay amplitude of the color-octet process can be written as

$$\begin{aligned}\mathcal{A}^{\text{real}}(b\bar{b}(^3S_{1,8}(2p_b)) \to c(p_c) + \bar{c}(p_{\bar{c}}) + g(k))|_{k^0<E_s} &= g_s\mu^\epsilon\varepsilon^a_{*\mu}(k)\left(\frac{p_c^\mu}{p_c\cdot k}T^a \otimes \mathcal{A}^{\text{Born}}\right. \\ &\quad - \mathcal{A}^{\text{Born}}\otimes T^a\frac{p_{\bar{c}}^\mu}{p_{\bar{c}}\cdot k} \\ &\quad \left. - \mathcal{A}^{\text{Born}}\frac{if^{ab_\Upsilon c_{c\bar{c}}}}{2}\frac{p_b^\mu}{p_b\cdot k}\right)\end{aligned} \tag{B17}$$

and

$$|\mathcal{A}^{\text{real}}(^3S_{1,8})|_{k^0<E_s}|^2 = |\mathcal{A}^{\text{Born}}(^3S_{1,8})|^2 g_s^2\mu^{2\epsilon}(\tfrac{4}{3}\mathcal{I}_{cc} + \tfrac{1}{3}\mathcal{I}_{c\bar{c}} + \tfrac{4}{3}\mathcal{I}_{\bar{c}\bar{c}} + 3\mathcal{I}_{bb} - 3\mathcal{I}_{bc} - 3\mathcal{I}_{b\bar{c}}). \tag{B18}$$

The integration of $\mathcal{I}_{ij}$ in the soft region with dimensional regularization can be found in Ref. [54], and with massive gluon can be found in Ref. [55]

APPENDIX C: THE TOTAL DECAY WIDTH

The decay width at NLO in α_s is

$$\Gamma_{\text{NLO}} = \Gamma_{\text{LO}} + \Gamma_{\text{virtual}} + \Gamma_{\text{real}}. \tag{C1}$$

The LO decay width of the color-singlet piece has been given in Eq. (6). The D-dimension LO decay width is

$$\Gamma_{\text{LO}}[\Upsilon(^3S_{1,1}) \to c\bar{c}] = \frac{4\pi\alpha^2\beta(D-2+r^2)}{81m_b^2}\frac{\sqrt{\pi}}{2\Gamma[\frac{3}{2}-\epsilon]} \times \left(\frac{4\pi\mu^2}{\beta^2 m_b^2}\right)^\epsilon \langle\Upsilon|\mathcal{O}(^3S_{1,1})|\Upsilon\rangle, \tag{C2}$$

where $r = m_c/m_b$ and $\beta = \sqrt{1-r^2}$.

The Γ_{virtual} of the color-singlet piece can be written as

$$\begin{aligned}\frac{\Gamma_{\text{virtual}}(^3S_{1,1})}{\Gamma_{\text{LO}}(^3S_{1,1})} &= \frac{\alpha_s}{\pi}\frac{r^2+2}{r^2+D-2}\left\{-4\left(\frac{1}{\epsilon} - \gamma_E + \ln\left(\frac{4\pi\mu^2}{m_b m_c}\right)\right) + \frac{16m_b^2}{3(2m_b^2+m_c^2)} - \frac{52}{9} + \frac{32i\pi^2}{9(2m_b^2+m_c^2)}\left[A_0(m_b)\left(4 - \frac{m_c^2}{m_b^2}\right)\right.\right. \\ &\quad - 3A_0(m_c) - 2(3B_0(p_c,0,m_c)(4m_b^2+m_c^2) + B_0(2p_b,m_b,m_b)(2m_b^2+m_c^2) - 3B_0(2p_b,m_c,m_c)(3m_b^2+m_c^2) \\ &\quad + 3B_0(p_b,0,m_b)m_b^2) + 12((D-2)m_b^2+m_c^2)(C_0(p_b,-p_{\bar{b}},0,m_b,m_b)m_b^2 \\ &\quad \left.\left. + C_0(p_c,-p_{\bar{c}},0,m_c,m_c)(2m_b^2-m_c^2))\right]\right\}.\end{aligned} \tag{C3}$$

For the real corrections, we should introduce the Mandelstam variables

$$s_{23} = (p_c + p_{\bar{c}})^2 \qquad s_{34} = (p_{\bar{c}} + k)^2. \tag{C4}$$

In the rest frame of Υ,

$$s_{23} = 4m_b^2 - 4m_b k^0 \qquad s_{34} = 4m_b^2 + m_c^2 - 4m_b p_c^0. \tag{C5}$$

The contribution of real corrections for the color-singlet piece is

$$\begin{aligned}\frac{d\Gamma_{\text{real}}(^3S_{1,1})}{dk^0 dp_c^0} &= -\frac{16\langle\Upsilon|\mathcal{O}(^3S_{1,1})|\Upsilon\rangle\alpha^2\alpha_s}{243m_b^4(m_c^2-s_{34})^2(-4m_b^2-m_c^2+s_{23}+s_{34})^2}\{2m_c^8 - 8s_{34}m_c^6 + (3s_{23}^2 + 4s_{34}s_{23} + 12s_{34}^2)m_c^4 \\ &\quad - (s_{23}^3 + 2s_{34}s_{23}^2 + 8s_{34}^2s_{23} + 8s_{34}^3)m_c^2 + 64m_b^6(3m_c^2 - s_{34}) + s_{34}(s_{23}+s_{34})(s_{23}^2 + 2s_{34}s_{23} + 2s_{34}^2) \\ &\quad + 16m_b^4[7m_c^4 - (5s_{23}+6s_{34})m_c^2 + s_{34}(s_{23}+3s_{34})] + 4m_b^2[4m_c^6 - 4(2s_{23}+3s_{34})m_c^4 \\ &\quad + (3s_{23}^2 + 4s_{34}s_{23} + 12s_{34}^2)m_c^2 - s_{34}(s_{23}+2s_{34})^2]\}.\end{aligned} \tag{C6}$$

The NLO decay width of the color-singlet piece is

$$\Gamma_{\rm NLO}[(^3S_{1,1})] = \frac{8\pi\alpha^2}{81m_b^2}\langle\Upsilon|\mathcal{O}(^3S_{1,1})|\Upsilon\rangle\bigg\{\sqrt{1-r^2}\bigg(1+\frac{r^2}{2}\bigg)\bigg(1-\frac{16\alpha_s}{4\pi}C_F\bigg)+\frac{\alpha_s}{4\pi}C_F\bigg[(32-8r^4)\mathrm{Li}_2(x_\beta)$$
$$+(16-4r^4)(\mathrm{Li}_2(-x_\beta)+\ln(x_\beta)\ln(1-x_\beta))+(2+r^2)\sqrt{1-r^2}(6\ln(x_\beta)-8\ln(1-x_\beta)-4\ln(1+x_\beta))$$
$$+\bigg(3+\frac{9r^2}{2}\bigg)\sqrt{1-r^2}+\bigg(-12+2r^2+\frac{7r^4}{4}\bigg)\ln(x_\beta)+(8-2r^4)\ln(x_\beta)\ln(1+x_\beta)\bigg]\bigg\}, \tag{C7}$$

where $\beta=\sqrt{1-r^2}$ and $x_\beta=(1-\beta)/(1+\beta)=(1-\sqrt{1-r^2})/(1+\sqrt{1-r^2})$. The $-\frac{16\alpha_s}{4\pi}C_F$ term is due to the QCD correction to $\Upsilon[b\bar{b}(^3S_{1,1})]\to\gamma^*$, while the $\frac{\alpha_s}{4\pi}C_F[\cdots]$ term is due to the QCD correction to $\gamma^*\to c\bar{c}$. This is the same as the known next-to-leading order result of $e^+e^-\to\gamma^*\to c\bar{c}$ [56,57].

The LO decay width of the color-octet piece has been given in Eq. (21). The D-dimension LO decay width is

$$\Gamma_{\rm LO}[\Upsilon(^3S_{1,8})\to c\bar{c}] = \frac{\alpha_s^2\beta(D-2+r^2)\pi}{6m_b^2}\frac{\sqrt{\pi}}{2\Gamma[\frac{3}{2}-\epsilon]}\bigg(\frac{4\pi\mu^2}{\beta^2m_b^2}\bigg)^\epsilon\langle\Upsilon|\mathcal{O}(^3S_{1,8})|\Upsilon\rangle. \tag{C8}$$

The $\Gamma_{\rm virtual}$ of the color-singlet piece can be written as

$$\frac{\Gamma_{\rm virtual}(^3S_{1,8})}{\Gamma_{\rm LO}(^3S_{1,8})} = \frac{\alpha_s(\mu)}{9\pi}\frac{r^2+2}{r^2+D-2}\bigg\{-\frac{147}{2}\bigg(\frac{1}{\epsilon}-\gamma_E+\ln(4\pi)\bigg)-18\log\bigg(\frac{\mu^4}{m_b^2m_c^2}\bigg)+\frac{202m_b^2-193m_c^2}{4(2m_b^2+m_c^2)}$$
$$+\frac{2i\pi^2}{m_b^2(2m_b^2+m_c^2)}[-A_0(m_b)(35m_b^2-2m_c^2)-12A_0(m_c)(6m_b^2+m_c^2)-15B_0(p_b,0,m_b)(7m_b^4+12m_c^2m_b^2)$$
$$-90B_0(2p_b,0,0)m_b^2(2m_b^2+m_c^2)+4B_0(2p_b,m_b,m_b)m_b^2(2m_b^2+m_c^2)+12B_0(2p_b,m_c,m_c)$$
$$\times(m_b^4+3m_c^2m_b^2+m_c^4)-96B_0(p_c,0,m_c)m_b^2(4m_b^2+m_c^2)-108B_0(p_b-p_c,m_b,m_c)m_b^4$$
$$-324C_0(p_b,-p_b,m_b,0,0)m_b^4(2m_b^2+m_c^2)-216C_0(p_c,-p_{\bar{c}},m_c,0,0)m_b^4(2m_b^2+m_c^2)$$
$$-24C_0(p_b,-p_{\bar{b}},0,m_b,m_b)m_b^4((D-2)m_b^2+m_c^2)-216C_0(p_c,p_b,0,m_c,m_b)m_b^4((D-2)m_b^2+m_c^2)$$
$$-24C_0(p_c,-p_{\bar{c}},0,m_c,m_c)m_b^2(2m_b^2-m_c^2)((D-2)m_b^2+m_c^2)$$
$$-432D_0(p_b,p_b-p_c,-p_b,m_b,0,m_c,0)m_b^6((D-2)m_b^2+m_c^2)]\bigg\}. \tag{C9}$$

The contribution of real corrections for the color-octet piece is

$$\frac{d\Gamma_{\rm real}(^3S_{1,8})}{dk^0dp_c^0} = -\frac{\langle\Upsilon|\mathcal{O}(^3S_{1,8})|\Upsilon\rangle\alpha_s^3}{18m_b^4(s_{23}-4m_b^2)^2(m_c^2-s_{34})^2(-4m_b^2-m_c^2+s_{23}+s_{34})^2}[64m_b^4+4(9m_c^2-8s_{23}-9s_{34})m_b^2+9m_c^4$$
$$+4s_{23}^2+9s_{34}^2+9s_{23}s_{34}-9m_c^2(s_{23}+2s_{34})]\{2m_c^8-8s_{34}m_c^6+(3s_{23}^2+4s_{34}s_{23}+12s_{34}^2)m_c^4$$
$$-(s_{23}^3+2s_{34}s_{23}^2+8s_{34}^2s_{23}+8s_{34}^3)m_c^2+64m_b^6(3m_c^2-s_{34})+s_{34}(s_{23}+s_{34})(s_{23}^2+2s_{34}s_{23}+2s_{34}^2)$$
$$+16m_b^4[7m_c^4-(5s_{23}+6s_{34})m_c^2+s_{34}(s_{23}+3s_{34})]+4m_b^2[4m_c^6-4(2s_{23}+3s_{34})m_c^4$$
$$+(3s_{23}^2+4s_{34}s_{23}+12s_{34}^2)m_c^2-s_{34}(s_{23}+2s_{34})^2]\}. \tag{C10}$$

The NLO decay width of the color-octet piece is

$$\Gamma_{\rm NLO}[(^3S_{1,8})] = \frac{\pi\alpha_s^2\langle\Upsilon|\mathcal{O}(^3S_{1,8})|\Upsilon\rangle}{6m_b^2}\beta(3-\beta^2) + \frac{\alpha_s^3\langle\Upsilon|\mathcal{O}(^3S_{1,8})|\Upsilon\rangle}{216m_b^2}\Big\{-12\beta^5 + 2\pi^2\beta^4 - 478\beta^3 + 14\pi^2\beta^2 + 1614\beta - 60\pi^2 - 150\beta(\beta^2-3)\ln\left(\frac{\mu^2}{m_b^2}\right) + 6(\beta^2-3)\ln(2)[90\beta + (\beta^2-17)\ln(2)] + 408\beta(\beta^2-3)\ln(\beta) - 6\beta(35\beta^2-87)\log(1-\beta^2) - 6(\beta^6 - 13\beta^4 + 4\beta^2 + 60)\log\left(\frac{1-\beta}{\beta+1}\right) + 6\log(\beta+1)[\log(2)\beta^4 - 5\log(16)\beta^2 + (-2\beta^4 + 31\beta^2 - 75)\log(\beta+1) + 51\log(2)] + 6\log(1-\beta)[-\log(8)\beta^4 + 60\log(2)\beta^2 + 3(\beta^4 - 20\beta^2 + 51)\log(\beta+1) - 153\log(2)] - 12(\beta^2-3)\Big[9\mathrm{Li}_2(\beta) + 9\mathrm{Li}_2\left(\frac{\beta}{\beta+1}\right) + (\beta^2-17)\left(2\mathrm{Li}_2\left(\frac{2\beta}{\beta+1}\right) - \mathrm{Li}_2\left(\frac{\beta+1}{2}\right)\right)\Big] - 12(\beta^4 - 20\beta^2 + 51)\log(\beta)\log\left(\frac{1-\beta}{\beta+1}\right)\Big\}. \tag{C11}$$

[1] G. T. Bodwin, E. Braaten, and G. P. Lepage, Phys. Rev. D **51**, 1125 (1995); **55**, 5853(E) (1997).
[2] M. Kramer, Nucl. Phys. **B459**, 3 (1996).
[3] M. Klasen, B. A. Kniehl, L. N. Mihaila, and M. Steinhauser, Phys. Rev. Lett. **89**, 032001 (2002).
[4] J. Abdallah *et al.* (DELPHI Collaboration), Phys. Lett. B **565**, 76 (2003).
[5] E. Braaten and J. Lee, Phys. Rev. D **67**, 054007 (2003); **72**, 099901(E) (2005).
[6] K. Y. Liu, Z. G. He, and K. T. Chao, Phys. Lett. B **557**, 45 (2003).
[7] K. Hagiwara, E. Kou, and C. F. Qiao, Phys. Lett. B **570**, 39 (2003).
[8] F. Yuan, C. F. Qiao, and K. T. Chao, Phys. Rev. D **56**, 321 (1997).
[9] K. Y. Liu, Z. G. He, and K. T. Chao, Phys. Rev. D **68**, 031501 (2003).
[10] K. Y. Liu, Z. G. He, and K. T. Chao, Phys. Rev. D **69**, 094027 (2004).
[11] K. Abe *et al.* (BELLE Collaboration), Phys. Rev. Lett. **89**, 142001 (2002).
[12] B. Aubert *et al.* (*BABAR* Collaboration), Phys. Rev. D **72**, 031101 (2005).
[13] Z. G. He, Y. Fan, and K. T. Chao, Phys. Rev. D **75**, 074011 (2007).
[14] G. T. Bodwin, D. Kang, and J. Lee, Phys. Rev. D **74**, 014014 (2006); **74**, 114028 (2006); G. T. Bodwin, J. Lee, and C. Yu, Phys. Rev. D **77**, 094018 (2008).
[15] Y. J. Zhang, Y. Q. Ma, and K. T. Chao, Phys. Rev. D **78**, 054006 (2008).
[16] Y. J. Zhang and K. T. Chao, Phys. Rev. Lett. **98**, 092003 (2007).
[17] Y. J. Zhang, Y. J. Gao, and K. T. Chao, Phys. Rev. Lett. **96**, 092001 (2006).
[18] B. Gong and J. X. Wang, Phys. Rev. Lett. **100**, 181803 (2008).
[19] B. Gong and J. X. Wang, Phys. Rev. D **77**, 054028 (2008).
[20] P. Artoisenet, J. P. Lansberg, and F. Maltoni, Phys. Lett. B **653**, 60 (2007).
[21] J. Campbell, F. Maltoni, and F. Tramontano, Phys. Rev. Lett. **98**, 252002 (2007).
[22] B. Gong, X. Q. Li, and J. X. Wang, arXiv:0805.4751.
[23] B. Gong and J. X. Wang, Phys. Rev. D **78**, 074011 (2008).
[24] B. Gong and J. X. Wang, Phys. Rev. Lett. **100**, 232001 (2008).
[25] N. Brambilla *et al.*, arXiv:hep-ph/0412158.
[26] J. P. Lansberg, Int. J. Mod. Phys. A **21**, 3857 (2006).
[27] J. P. Lansberg *et al.*, AIP Conf. Proc. **1038**, 15 (2008).
[28] H. Fritzsch and K. H. Streng, Phys. Lett. B **77**, 299 (1978).
[29] I. I. Y. Bigi and S. Nussinov, Phys. Lett. B **82**, 281 (1979).
[30] R. Barbieri, M. Caffo, and E. Remiddi, Phys. Lett. **83B**, 345 (1979).
[31] F. Maltoni and A. Petrelli, Phys. Rev. D **59**, 074006 (1999).
[32] G. T. Bodwin, E. Braaten, D. Kang, and J. Lee, Phys. Rev. D **76**, 054001 (2007).
[33] Y. J. Gao, Y. J. Zhang, and K. T. Chao, arXiv:hep-ph/0701009.
[34] Y. J. Gao, Y. J. Zhang, and K. T. Chao, Chin. Phys. Lett. **23**, 2376 (2006).
[35] Y. J. Gao, Y. J. Zhang, and K. T. Chao, Commun. Theor. Phys. **46**, 1017 (2006).
[36] A. Petrelli, M. Cacciari, M. Greco, F. Maltoni, and M. L. Mangano, Nucl. Phys. **B514**, 245 (1998).
[37] G. T. Bodwin and A. Petrelli, Phys. Rev. D **66**, 094011 (2002).
[38] Y. Jia, Phys. Rev. D **76**, 074007 (2007).
[39] D. Kang, T. Kim, J. Lee, and C. Yu, Phys. Rev. D **76**, 114018 (2007).
[40] H. S. Chung, T. Kim, and J. Lee, arXiv:0805.1989.
[41] G. Hao, C. F. Qiao, and P. Sun, Phys. Rev. D **76**, 125013 (2007).
[42] H. Albrecht *et al.* (ARGUS Collaboration), Z. Phys. C **55**, 25 (1992).
[43] R. A. Briere *et al.* (CLEO Collaboration), Phys. Rev. D **78**, 092007 (2008).
[44] J. Kublbeck, M. Bohm, and A. Denner, Comput. Phys. Commun. **60**, 165 (1990).

[45] T. Hahn, Comput. Phys. Commun. **140**, 418 (2001).
[46] R. Mertig, M. Bohm, and A. Denner, Comput. Phys. Commun. **64**, 345 (1991).
[47] T. Hahn and M. Perez-Victoria, Comput. Phys. Commun. **118**, 153 (1999).
[48] J. H. Kuhn, J. Kaplan, and E. G. O. Safiani, Nucl. Phys. **B157**, 125 (1979).
[49] B. Guberina, J. H. Kuhn, R. D. Peccei, and R. Ruckl, Nucl. Phys. **B174**, 317 (1980).
[50] W. M. Yao *et al.* (Particle Data Group), J. Phys. G **33**, 1 (2006).
[51] P. M. Stevenson, Phys. Lett. **100B**, 61 (1981); P. M. Stevenson, Phys. Rev. D **23**, 2916 (1981).
[52] G. T. Bodwin, J. Lee, and D. K. Sinclair, Phys. Rev. D **72**, 014009 (2005).
[53] Yu-Jie Zhang, Ph.D. thesis, School of Physics, Peking University, 2007.
[54] B. W. Harris and J. F. Owens, Phys. Rev. D **65**, 094032 (2002).
[55] G. 't Hooft and M. J. G. Veltman, Nucl. Phys. **B153**, 365 (1979).
[56] J. Jersak, E. Laermann, and P. M. Zerwas, Phys. Rev. D **25**, 1218 (1982); **36**, 310(E) (1987).
[57] V. Ravindran and W. L. van Neerven, Phys. Lett. B **445**, 206 (1998).